J. Fluid Mech. (1993), *vol.* 255, *pp.* 301–321

Convective stability of gravity-modulated doubly cross-diffusive fluid layers

By GUILLERMO TERRONES[1] AND C. F. CHEN[2]

[1] Analytic Sciences Department, Battelle Pacific Northwest Laboratories, Richland, WA 99352, USA

[2] Department of Aerospace and Mechanical Engineering The University of Arizona, Tucson, AZ 85721, USA

(Received 17 April 1992 and in revised form 8 February 1993)

A stability analysis is undertaken to theoretically study the effects of gravity modulation and cross-diffusion on the onset of convection in horizontally unbounded doubly diffusive fluid layers. We investigate the stability of doubly stratified incompressible Boussinesq fluid layers with stress-free and rigid boundaries when the stratification is either imposed or induced by Soret separation. The stability criteria are established by way of Floquet multipliers of the amplitude equations. The topology of neutral curves and stability boundaries exhibits features not found in modulated singly diffusive or unmodulated multiply diffusive fluid layers. A striking feature in gravity-modulated doubly cross-diffusive layers is the existence of bifurcating neutral curves with double minima, one of which corresponds to a quasi-periodic asymptotically stable branch and the other to a subharmonic neutral solution. As a consequence, a temporally and spatially quasi-periodic bifurcation from the basic state is possible, in which case there are two incommensurate critical wavenumbers at two incommensurate onset frequencies at the same Rayleigh number. In some instances, the minimum of the subharmonic branch is more sensitive to small parameter variations than that of the quasi-periodic branch, thus affecting the stability criteria in a way that differs substantially from that of unmodulated layers.

1. Introduction

During directional solidification of a molten alloy by cooling from below, solutes are rejected through a crystallization process leading to the development of temperature and concentration gradients (McFadden *et al.* 1984). The distribution of these stratifying agencies may overturn the melt and might adversely affect material properties of the castings. It has been argued that the solute redistribution caused by buoyancy-driven convection can be substantially reduced by processing materials on board orbiting laboratories in spacecraft where the mean gravity field is at least four orders of magnitude smaller than its value g_0 on the Earth's surface.

Owing to several unavoidable sources of residual acceleration experienced by a spacecraft (Nelson 1991), the gravity field in an orbiting laboratory is not constant in a microgravity environment but is, rather, a randomly fluctuating field in magnitude and direction, which is referred to as g-jitter. Typical g-jitter ranges for frequency, amplitude, and mean are $(10^{-2}$–$10^{3})$ Hz, $(10^{-5}$–$10^{-4})\ g_0$, and $(10^{-5}$–$10^{-4})\ g_0$, respectively. The literature on the effects of g-jitter in materials processing is quite extensive; for a recent comprehensive review the reader is referred to Nelson (1991). In this paper, we consider how the onset of convection in horizontal doubly cross-diffusive fluid layer

systems is affected by a time-dependent sinusoidal gravity field perpendicular to the lateral boundaries of the fluid layer.

In general, a distribution of stratifying agencies that is convectively stable under constant gravity conditions can be destabilized when a time-dependent component of the gravity field is introduced. The effect of gravity modulation on a convectively stable configuration can significantly influence the stability of a system by increasing or decreasing its susceptibility to convection. This added new way of controlling the stability of a system is dependent upon the magnitude of the amplitude and frequency of the modulation. Furthermore, in a multiply diffusive system, the coupling among the various stratifying agencies manifested in cross-diffusion effects can strongly affect the convective stability of the layer (McDougall 1983; Platten & Legros 1984; Henry 1990; Terrones 1993). Suitable combinations of stratification gradients, physical properties and modulation parameters may lead to parametric resonance and hence to instability of the system.

Gershuni, Zhukhovitskii & Iurkov (1970) and Gresho & Sani (1970) studied the onset of convection in a singly diffusive vertically oscillated fluid layer with rigid boundaries. In both of these studies, a single trial function was used to construct the stability boundaries. The former authors performed a thorough study and obtained more accurate results than the latter; however, they reported incomplete neutral curves, lacking the subharmonic branches. In addition to the unbounded fluid layer configuration, Wadih & Roux (1988) and Wadith, Zahibo & Roux (1990) studied the effect of small-amplitude gravity modulation on convection in long cylindrical cavities. A full Navier–Stokes simulation of the Bénard problem in a finite box was done by Biringen & Peltier (1990). The results of these authors agreed with the stability calculations of Gresho & Sani (1970). Murray, Coriell & McFadden (1991) considered the effect of gravity modulation on the onset of convection for the unidirectional solidification problem. Wheeler *et al.* (1991) analysed the same problem in the high-frequency modulation limit. More recently, Saunders *et al.* (1992) studied the onset of convection in a gravity-modulated doubly diffusive fluid layer with stress-free boundaries and no cross-diffusion. Their efforts concentrated on the construction of planar boundaries of convective stability spanned by the relative amplitude and the inverse of the modulation frequency. They found that for diffusive-like configurations the regions of resonant instability are strongly coupled with multiples of the corresponding onset frequencies in the absence of modulation.

This paper is devoted to the study of the effects of a modulated vertical gravity field (not restricted to an analysis for small gravity-modulation amplitude) in doubly diffusive layers with and without cross-diffusion and by considering stress-free and rigid boundary conditions. Attention is focused on the determination of the linear stability criteria for such systems. Using Floquet theory (Yakubovich & Starzhinskii 1975), the stability criteria are established by a systematic analysis of the topology of the neutral curves from which stability boundaries are constructed. Boundaries of convective stability for gravity-modulated doubly cross-diffusive systems are presented herein for the cases of dynamically free and rigid boundaries. In both cases, two physically different forms of layer stratification are considered: (i) imposed independent stratification of two components (with and without cross-diffusion), and (ii) a solute distribution induced by a fixed temperature gradient (Soret separation).

Gravity-modulation and cross-diffusion effects in doubly diffusive systems lead to a wide variety of topologically complex boundaries of convective stability. These can be composed of up to three kinds of asymptotically stable neutral solutions, namely, synchronous, subharmonic, and quasi-periodic. A remarkable departure from gravity-

modulated singly diffusive fluid layers is the possibility of a quasi-periodic bifurcation in time and in space from the motionless basic state. This bifurcation can take place in configurations with either stress-free or rigid boundaries.

2. Linear stability analysis

Unbounded incompressible horizontal fluid layers of depth d under the influence of a periodically varying vertical gravity field in which the fluid density depends on two stratifying agencies with different rates of diffusion and cross-diffusion are considered. Cross-diffusion is incorporated into the conservation equation by assuming that the contribution to the fluxes of the components can be expressed as linear combinations of gradients of the stratifying agencies (generalized Fick–Fourier law of diffusion);

$$J_m = -\sum_{k=1}^{2} \rho D_{mk} \nabla r_k, \quad m = 1, 2,$$

where ρ is the density of the fluid mixture, D_{mk} is the diffusivity matrix, and r_k is the kth stratifying agency of the system. This expression is valid as long as the temperature and concentration gradients in the fluid layer are not exceedingly high (De Groot 1952).

Within the Boussinesq approximation the continuity, momentum, and conservation equations in dimensional form are, respectively,

$$\frac{\partial v_i}{\partial \xi_i} = 0,$$

$$\frac{\partial v_i}{\partial \tau} + v_j \frac{\partial v_i}{\partial \xi_j} = -\frac{1}{\rho_0}\frac{\partial p}{\partial \xi_i} - \frac{\rho}{\rho_0} g \delta_{i3} + \nu \frac{\partial^2 v_i}{\partial \xi_j \partial \xi_j}, \quad i,j = 1,2,3,$$

$$\frac{\partial r_m}{\partial \tau} + v_j \frac{\partial r_m}{\partial \xi_j} = \frac{\partial}{\partial \xi_j}\left(D_{mk}\frac{\partial r_k}{\partial \xi_j}\right), \quad m = 1, 2,$$

where v_i are the velocity components, τ is the time variable, ξ_i are spatial coordinates, g is a periodic function of time, ρ_0 is a reference fluid density, and ν is the kinematic viscosity.

The density is a linear function of two stratifying agencies

$$\rho = \rho_0\left[1 + \sum_{m=1}^{2} \beta_m (r_m - q_m)\right], \qquad \beta_m = \frac{1}{\rho_0}\left(\frac{\partial \rho}{\partial r_m}\right)_{r_j, p}, \quad j \neq m = 1, 2,$$

where q_m is the value of the mth stratifying agency at the bottom of the layer, and β_m is the mth isobaric expansion coefficient. The governing equations admit a motionless basic-state solution in which the distributions of the stratifying agencies are linear in the vertical coordinate.

Gershuni *et al.* (1970) and Gresho & Sani (1970) expressed the gravity-modulation amplitude as a function of the frequency and the maximum displacement of a shaker table. However, in a microgravity environment the time-dependent gravity fluctuations can be described by a typical g-jitter amplitude and frequency rather than a displacement. Following Wadih & Roux (1988), we separate the frequency dependence $\bar{\Omega}$ from the gravity-modulation amplitude g_1', and write

$$g(\tau) = g_0 + g_1' \cos(\bar{\Omega}\tau).$$

For convenience, we split the modulation amplitude ($g_1' = hg_1$) into a dimensionless factor h and a dimensional number g_1 (not necessarily equal to the mean gravity field g_0). This separation allows a more general non-dimensionalization in which we avoid the occurrence of singular parameters for vanishing values of either g_0 or g_1'. By setting h to zero, we can validate our results with the unmodulated fluid layer problem. In addition, we only need to define one Rayleigh number (based on g_1) for each component in the fluid layer.

We define the non-dimensional independent variables,

$$x_i = \xi_i/\mathrm{d}, \quad t = D_{11}\tau/\mathrm{d}^2,$$

and dependent perturbation variables,

$$u_i = \frac{dv_i}{D_{11}}, \quad P = \frac{d^2p}{\rho_0 \nu D_{11}}, \quad S_m = \frac{g_1 \beta_m d^3 r_m}{\nu D_{11}}$$

along with the non-dimensional parameters,

$$R_m = g_1 \beta_m d^3 \Delta q_m / \nu D_{11}, \quad Pr = \nu / D_{11},$$

$$\Omega = \frac{d^2\bar{\Omega}}{D_{11}}, \quad f = \frac{g_0}{g_1}, \quad h = \frac{g_1'}{g_1}, \quad \gamma_{mk} = \frac{\beta_m D_{mk}}{\beta_k D_{11}}, \quad Sr = -\frac{\gamma_{21}}{\gamma_{22}},$$

where R_m is the Rayleigh number of the mth stratifying agency, Pr is a generalized Prandtl number, which in the case of isothermal ternary mixtures becomes a Schmidt number, Ω is the dimensionless modulation frequency, f is the scaled mean-to-amplitude gravity ratio, h is an amplitude magnification factor, γ_{mk} are the diffusivity-expansion coefficient ratios, and Sr is the Soret number or separation ratio. According to our convention, a positive R_m means that the mth component is destabilizing. Because of the one-dimensionality of the basic state and the horizontal isotropy of the problem, the analysis is restricted to two-dimensional motions. Thus, a perturbation stream function ψ is introduced,

$$u = \frac{\partial \Psi}{\partial z}, \quad w = -\frac{\partial \Psi}{\partial x}.$$

We obtain the linearized perturbation equations

$$\frac{1}{Pr}\frac{\partial}{\partial t}\nabla^2\Psi - \nabla^4\Psi = (f + h\cos\Omega t)\left(\frac{\partial S_1}{\partial x} + \frac{\partial S_2}{\partial x}\right), \tag{2.1}$$

$$\frac{\partial S_1}{\partial t} = \nabla^2 S_1 + \gamma_{12}\nabla^2 S_2 + R_1\frac{\partial \Psi}{\partial x}, \tag{2.2}$$

$$\frac{\partial S_2}{\partial t} = \gamma_{21}\nabla^2 S_1 + \gamma_{22}\nabla^2 S_2 + R_2\frac{\partial \Psi}{\partial x}, \tag{2.3}$$

to which we append the following boundary conditions at $z = \frac{1}{2}\epsilon - 1, \frac{1}{2}\epsilon$:

$$S_1 = S_2 = \Psi = \frac{\partial^\epsilon \Psi}{\partial z^\epsilon} = 0, \tag{2.4}$$

where $\epsilon = 1$ corresponds to rigid–rigid boundaries and $\epsilon = 2$ to free–free boundaries. Note that in the case of rigid boundaries, the origin of the coordinate system has been shifted to a plane midway between the boundaries.

The case of stress-free boundaries is mathematically simpler due to the separability of the perturbation equations for normal disturbances that satisfy the homogeneous boundary conditions (2.4) for $\epsilon = 2$. The perturbation stream function and concentrations can be written as

$$\begin{Bmatrix} \Psi(x,z,t) \\ S_1(x,z,t) \\ S_2(x,z,t) \end{Bmatrix} = \begin{Bmatrix} a(t) \\ b(t) \\ c(t) \end{Bmatrix} \sin(n\pi z)\, e^{ikx},$$

where k is the dimensionless horizontal wavenumber. Considering the fundamental (most unstable) mode of instability, and the following change of variables:

$$t = \frac{\theta}{\pi^2 + k^2}, \quad a(t) = A(\theta), \quad b(t) = \frac{kB(\theta)}{\pi^2 + k^2}, \quad c(t) = \frac{kC(\theta)}{\pi^2 + k^2},$$

equations (2.1)–(2.3) are reduced to a system of three ordinary differential equations with periodic coefficients (ODEPC) for the perturbation amplitudes:

$$\frac{dA}{d\theta} = -Pr\, A + \frac{Pr\, k^2}{(\pi^2 + k^2)^3}\left[f + h\cos\left(\frac{\Omega\theta}{\pi^2 + k^2}\right)\right](B + C),$$

$$\frac{dB}{d\theta} = R_1 A - B - \gamma_{12} C, \quad \frac{dC}{d\theta} = R_2 A - \gamma_{21} B - \gamma_{22} C.$$

For rigid boundaries we expand the disturbances in terms of a complete set of trial functions:

$$\Psi(x,z,t) = \sum_{n=1}^{N} a_n(t)\, \hat{\Psi}_n(z)\, e^{ikx}, \tag{2.5}$$

$$S_1(x,z,t) = \sum_{n=1}^{N} b_n(t)\, \hat{S}_n(z)\, e^{ikx}, \tag{2.6}$$

$$S_2(x,z,t) = \sum_{n=1}^{N} c_n(t)\, \hat{S}_n(z)\, e^{ikx}. \tag{2.7}$$

The presence of the bi-Laplacian of the stream function in (2.1), suggests the choice of trial functions that satisfy a fourth-order eigenvalue problem, leading to an orthonormal set of trial functions in the vertical direction (Chandrasekhar 1961).

$$\hat{\Psi}_n(z) = \begin{cases} \dfrac{\cosh(\eta_n z)}{\cosh(\frac{1}{2}\eta_n)} - \dfrac{\cos(\eta_n z)}{\cos(\frac{1}{2}\eta_n)}, & \tanh(\frac{1}{2}\eta_n) + \tan(\frac{1}{2}\eta_n) = 0, \quad n \text{ odd} \\ \dfrac{\sinh(\eta_n z)}{\sinh(\frac{1}{2}\eta_n)} - \dfrac{\sin(\eta_n z)}{\sin(\frac{1}{2}\eta_n)}, & \coth(\frac{1}{2}\eta_n) + \cot(\frac{1}{2}\eta_n) = 0, \quad n \text{ even.} \end{cases} \tag{2.8}$$

Since the highest-order spatial derivatives for perturbations of the stratifying agencies are second order, the trigonometric trial functions

$$\hat{S}_n(z) = \begin{cases} \cos(n\pi z) & n \text{ odd} \\ \sin(n\pi z) & n \text{ even} \end{cases} \tag{2.9}$$

will form a complete set since they satisfy homogeneous boundary conditions as well.

We substitute into (2.1)–(2.3) the truncated series expansions (2.5)–(2.7) together with (2.8) and (2.9) and use the Galerkin method. Finally, the amplitude equations are obtained as an implicit system of ODEPCs:

$$\begin{bmatrix} C_{ji}Pr^{-1} & 0 & 0 \\ 0 & -F_{ji} & 0 \\ 0 & 0 & -F_{ji} \end{bmatrix} \frac{\mathrm{d}}{\mathrm{d}t} \begin{Bmatrix} a_i \\ b_i \\ c_i \end{Bmatrix}$$

$$= \begin{bmatrix} -D_{ji} & (f+h\cos\Omega t)k^2E_{ji} & (f+h\cos\Omega t)k^2E_{ji} \\ R_1H_{ji} & -G_{ji} & -\gamma_{12}G_{ji} \\ R_2H_{ji} & -\gamma_{21}G_{ji} & -\gamma_{22}G_{ji} \end{bmatrix} \begin{Bmatrix} a_i \\ b_i \\ c_i \end{Bmatrix}, \quad (2.10)$$

where the inner products

$$\langle F, G\rangle = \int_{-\frac{1}{2}}^{\frac{1}{2}} FG\,\mathrm{d}z,$$

$$C_{ji} = -\left\langle \hat{\Psi}_j, \left(\frac{\mathrm{d}^2}{\mathrm{d}z^2} - k^2\right)\hat{\Psi}_i \right\rangle, \quad D_{ji} = \left\langle \hat{\Psi}_j, \left(\frac{\mathrm{d}^2}{\mathrm{d}z^2} - k^2\right)^2 \hat{\Psi}_i \right\rangle,$$

$$G_{ji} = -\left\langle \hat{S}_j, \left(\frac{\mathrm{d}^2}{\mathrm{d}z^2} - k^2\right)\hat{S}_i \right\rangle, \quad E_{ji} = \langle \hat{\Psi}_j, \hat{S}_i\rangle = H_{ij}, \quad F_{ji} = \langle \hat{S}_j, \hat{S}_i\rangle$$

can be easily represented in closed form. Note that the matrix in the right-hand side of (2.10) is a $2\pi/\Omega$-periodic matrix-function of time.

3. Neutral curves and stability boundaries

The first step in determining boundaries of convective stability is finding asymptotically stable neutral solutions of the amplitude equations. According to Floquet theory, a normal solution vector $\boldsymbol{\phi}(t)$ of a $\mathscr{T}$-periodic ($\mathscr{T} = 2\pi/\Omega$) first-order linear system of ODEPCs can be written as

$$\boldsymbol{\phi}(t) = \mathrm{e}^{\alpha t}\boldsymbol{\Phi}(t)$$

where $\alpha = \alpha_R + \mathrm{i}\alpha_I$ are the characteristic exponents and $\boldsymbol{\Phi}$ is a $\mathscr{T}$-periodic vector function. Thus, the asymptotic stability of a solution $\boldsymbol{\phi}(t)$ is determined by the real part of the most unstable characteristic exponent $\alpha_{R,max}$. $\boldsymbol{\phi}(t)$ is stable if $\alpha_{R,max} < 0$, and neutrally stable if $\alpha_{R,max} = 0$.

In the most general case of gravity-modulated doubly cross-diffusive fluid layers, the critical Rayleigh number depends on nine independent parameters. For brevity, we will lump these parameters into a vector $\boldsymbol{P}$:

$$\boldsymbol{P} = (R_2, \gamma_{12}, \gamma_{21}, \gamma_{22}, Pr, h, f, \Omega, k),$$

$$R_{1,crit} = F(\boldsymbol{P}).$$

Depending on the values of $\boldsymbol{P}$, solutions of the amplitude equations can be damped, amplified or neutral in time. As recognized by Saunders *et al.* (1992), the stability criteria are dependent upon a large number of dimensionless groups. Consequently, only projections of the global stability boundary over a limited range of the parameter vector $\boldsymbol{P}$ can be graphically represented. The task of finding neutral solutions can be considerably simplified by fixing eight parameters in $\boldsymbol{P}$, thus reducing the search from

a ten-dimensional space to a plane. By maintaining both stratifying agencies constant, Saunders *et al.* (1992) presented their stability results in the relative amplitude *vs.* inverse modulation frequency plane. Instead, we start by constructing a series of neutral curves in the (R_i, k)-plane. Once the topology of neutral curves and the critical Rayleigh numbers are determined, stability boundaries in the (R_1, R_2)- and (R_1, Sr)-planes are generated.

To locate marginally stable points in the (R_1, k)-plane we used wavenumber traverses by fixing the wavenumber and varying R_1 successively. In the case of either rigid or impervious (zero mass flux) boundaries, for an Mth order truncation of the perturbation variables, a fundamental matrix is obtained at each (k, R_1) point by integrating a system of $3M$ amplitude equations (with linearly independent initial conditions) $3M$ times. The monodromy matrix is obtained after the amplitude equations have been integrated in time up to one full period of the modulation. Computation of the eigenvalues of the monodromy matrix renders a set of Floquet multipliers χ from which we calculate the characteristic exponents ($\alpha = [\ln \chi]/\mathscr{T}$). We obtain marginally stable points on the neural curves by adjusting R_1 to drive the real part of the most unstable characteristic exponent to zero.

After an extremal Rayleigh number is found an R_1 horizontal traverse is performed to search for different neutral curves. If no other branch is found, the extremal Rayleigh number is critical, otherwise another extremum must be computed until a critical value is attained. The type of asymptotically stable neutral solution, namely synchronous, subharmonic or quasi-periodic, is determined by the value of $\alpha_{I,N}$ the imaginary part of the characteristic exponent for which $\alpha_{R,max} = 0$. If $\alpha_{I,N} = n\Omega$ $(n = 0, 1, 2, \ldots)$ the neutral solution $\boldsymbol{\phi}_N(t)$ is synchronous. If $\alpha_{I,N} = \frac{1}{2}(1+2n)\Omega$, then $\boldsymbol{\phi}_N(t)$ is subharmonic. If $\alpha_{I,N} = \frac{1}{2}\kappa\Omega$, $(|\kappa| \neq n)$, then $\boldsymbol{\phi}_N(t)$ is quasi-periodic because it is the product of two functions ($e^{i\alpha_{I,N}t}$ and $\boldsymbol{\Phi}$) whose frequencies ($\frac{1}{2}\kappa\Omega$ and Ω) are incommensurate.

Proceeding as above, the topology of neutral curves is determined in the (R_1, k)-plane. However, in order to construct a stability boundary in the (R_1, x)-plane (where x is a dimensionless group in P different from k) a family of (R_1, k) curves parametrized by x must be generated. In general, for each x there is a set of neutral curves in the (R_1, k)-plane that belongs to different solutions of the amplitude equations. The relative locations of these curves determines a set of critical Rayleigh numbers which constitute the points of the stability boundary in the (R_1, x)-plane. In particular, we choose x to be R_2 and Sr.

It is worth remarking that the even and odd trial functions are not coupled because of the even symmetry of the boundary conditions with respect to our coordinate system and also the linearity of the amplitude equations. The separation of even and odd functions also takes place in the unmodulated singly diffusive case as pointed out by Chandrasekhar (1961). Gresho & Sani (1970) realized that in the modulated case, odd solutions are not associated with the lowest Rayleigh number and thus can be discarded.

4. Results and discussion

The results discussed herein show fundamentally different features in the topology of neutral curves and stability boundaries that are not found in modulated singly diffusive systems or unmodulated multiply diffusive systems (Turner 1985; Pearlstein, Harris & Terrones 1989; Terrones & Pearlstein 1989; Lopez, Romero & Pearlstein 1990; Terrones 1993). Results in this section are classified into the following groups:

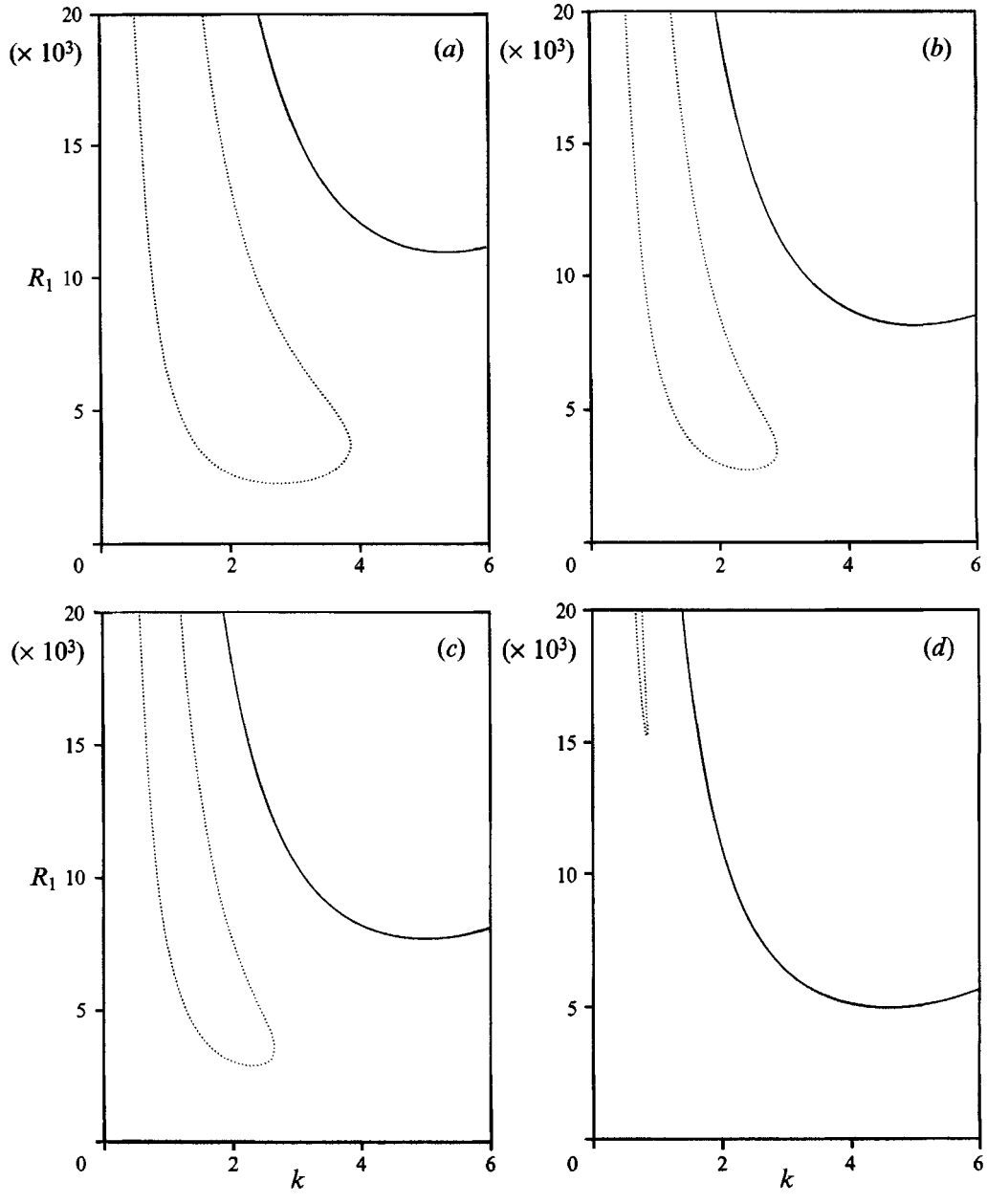

FIGURE 1. Effect of modulation frequency on neutral curves for a gravity-modulated singly diffusive layer with rigid boundaries. $Pr = 7.1, f = 1, h = 5$. · · · · ·, Synchronous branch; ——, subharmonic branch. (*a*) $\Omega = 500$, (*b*) $\Omega = 400$, (*c*) $\Omega = 375$, (*d*) $\Omega = 250$.

(i) singly diffusive stratification; (ii) imposed doubly diffusive stratification in which both gradients of the stratifying agencies are independent of each other; (iii) imposed doubly cross-diffusive stratification; and (iv) induced doubly diffusive stratification in non-isothermal layers (Soret separation).

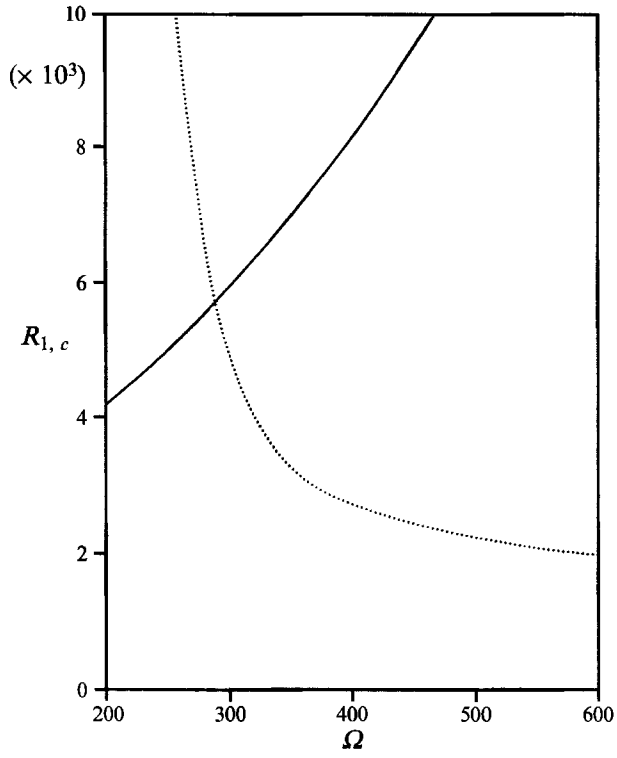

FIGURE 2. Critical Rayleigh numbers as a function of the dimensionless modulation frequency Ω for rigid boundaries. $Pr = 7.1, f = 1, h = 5$. · · · · ·, Synchronous branch; ——, subharmonic branch.

4.1. *Singly diffusive stratification*

The modulated single-component layer with impervious boundaries was studied for code-validation purposes. Although this case has previously been analysed by several authors, Gershuni *et al.* (1970) reported incomplete neutral curves by overlooking the synchronous branches in their Rayleigh number *vs.* wavenumber neutral curves (figure 5 in their paper). Neutral curves in the (R_1, k)-plane for four dimensionless modulation frequencies decreasing from $\Omega = 500$ to 250 are shown in figure 1 (*a–d*). The existence of subharmonic neutral curves precludes full stabilization because for decreasing values of Ω the synchronous extremum increases (stabilizing the layer) while the subharmonic extremum decreases, becoming eventually the critical Rayleigh number.

Figure 2 shows the synchronous and subharmonic critical Rayleigh numbers as a function of Ω. For increasing values of Ω, the subharmonic branch intersects the synchronous branch, at which point the instability mode changes. Note that because we used a different non-dimensionalization than Gresho & Sani (1970), their figure 4, does not match our figure 2. They fixed δFr which in our nomenclature corresponds to h/Ω^2. When they increased Ω, they automatically increased the amplitude factor h in order to keep δFr constant. We fixed h and increased Ω, so in Gresho & Sani's language, we decreased their δFr. A point-by-point comparison can be made between the figures. For example, we used $h = 5$, while they set $\delta Fr = 10^{-5}$. For these values Ω is about 700. We obtained a critical Rayleigh number (that belongs to a synchronous neutral curve) of 1955.4 and a critical wavenumber of 2.93, which are in excellent agreement with Gresho and Sani's results (their figure 4 should read $R_c \times 10^{-3}$ instead

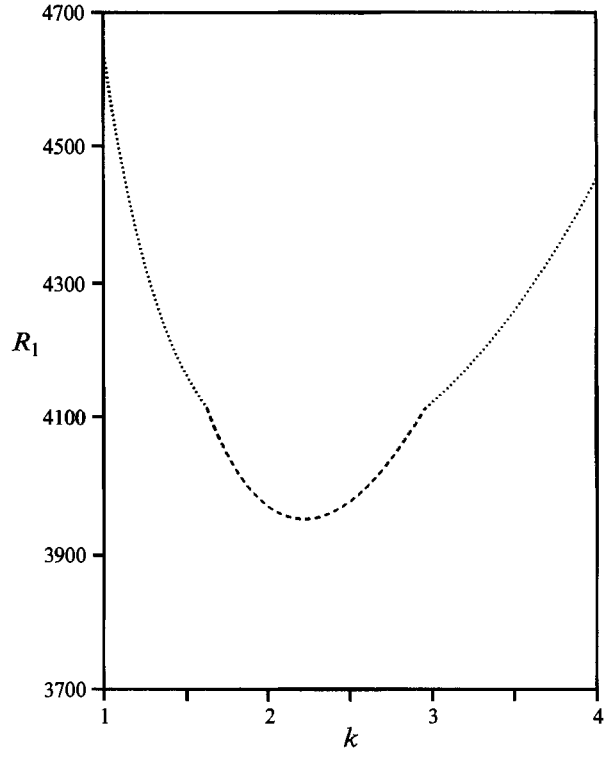

FIGURE 3. Neutral curve for a doubly diffusive fluid layer with stress-free boundaries under constantgravity. $Pr = 7$, $\gamma_{22} = 0.8$, $R_2 = -2700$, $f = 1$, $h = 0$. · · · · ·, Steady branch; ——, oscillatory branch.

of $R_c \times 10^{-5}$). Our computations show that all of the qualitative features of these results also apply to stress-free boundaries.

4.2. *Imposed doubly diffusive stratification*

In an unmodulated doubly diffusive fluid layer, elements of the coefficient matrix in the linearized perturbation equations are constant. Since any constant function is a periodic function of arbitrary period, Floquet theory is clearly applicable to the unmodulated stability problem. The characteristic exponents α become the growth rates of a matrix eigenvalue problem and validation of our code with the unmodulated fluid layers (see Appendix) was possible.

Figure 3 shows a neutral curve for an unmodulated doubly diffusive layer with stress-free boundaries generated by setting $h = 0$. The growth rates, computed according to Floquet theory, agreed with those obtained analytically for a constant gravity field. This case is representative of the most complex topology of a neutral curve in unmodulated doubly diffusive systems, namely an oscillatory branch connected by two bifurcation points to a steady neutral curve. The value of $\gamma_{22} = 0.8$ was specially chosen so that these bifurcation points are located at a value of R_1 not too different from the critical one.

In figure 4(*a*, *b*), for the same thermophysical parameters, gravity modulation is introduced and a banana-shaped subharmonic branch bifurcates from a quasi-periodic branch. Note that even though the upper branches in figures 3 and 4 may look the same, they represent different classes of solutions. The upper (dotted) branch in figure

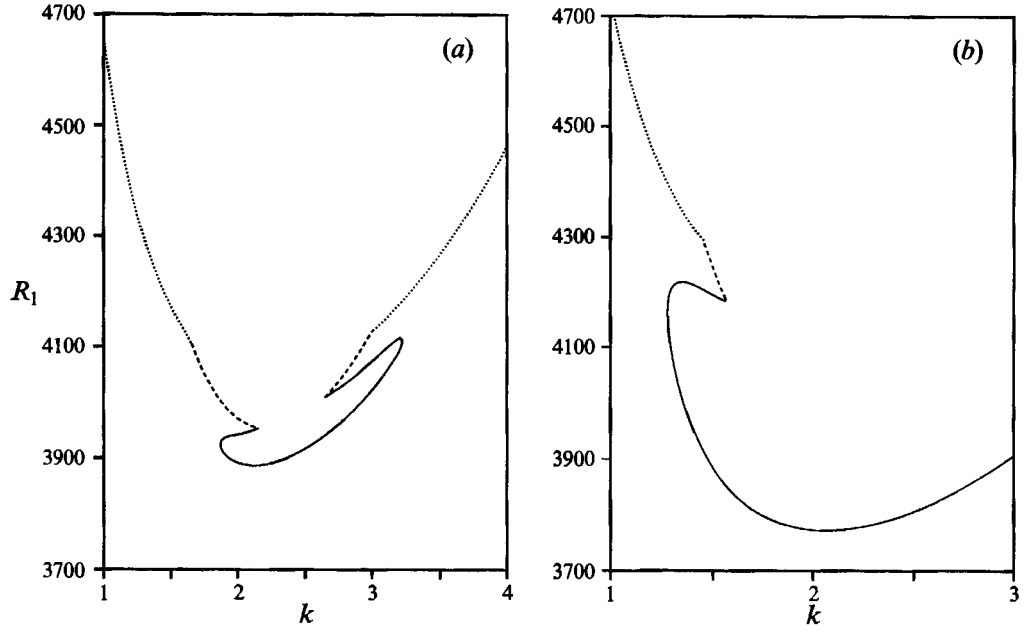

FIGURE 4. Effect of modulation amplitude on neutral curves for a gravity-modulated stress-free doubly diffusive layer. $Pr = 7$, $\gamma_{22} = 0.8$, $R_2 = -2700$, $f = 1$, $\Omega = 10$. · · · · ·, Synchronous branch; – – –, quasi-periodic branch; ——, subharmonic branch. (*a*) $h = 0.1$, (*b*) $h = 0.5$.

R_2	−3000	−4000	−5000	−6000
$R_{1,QP}$	708.2	718.2	728.4	738.3
$R_{1,SH}$	2313.5	92.4	−198.0	−337.4
k_{QP}	2.22	2.22	2.22	2.22
k_{SH}	6.62	4.05	3.13	2.65
ω_{QP}	3.15, 10.00	3.64, 10.00	4.06, 10.00	4.46, 10.00
ω_{SH}	5.00	5.00	5.00	5.00

TABLE 1. Gravity-modulated doubly diffusive stress-free fluid layer for which double minima exist. $Pr = 10^{-2}$, $\gamma_{21} = 3 \times 10^{-4}$, $f = 1$, $h = 0.1$, $\Omega = 10$. QP, Quasi-periodic; SH, subharmonic

4(*a*) represents periodic disturbances exhibiting a synchronous temporal response, whereas the upper branch in figure 3 represents steady disturbances. Increasing the amplitude of the modulation h causes the subharmonic branch to grow in all directions. This lowers the critical Rayleigh number and therefore makes the layer more unstable. This is shown in figure 4(*b*), where the onset of convection is via subharmonic disturbances.

In the examples discussed so far, the parameters are appropriate for aqueous salt solutions. For materials processing involving liquid metals, the Prandtl number is on the order of 10^{-2} and Schmidt numbers vary between 10^1 and 10^3. In the results that follow, we used typical liquid-metal physical properties of binary tin-based alloys with a diffusivity ratio of 3×10^{-4} and a Schmidt number of 34 (Henry 1990). An interesting feature in this range is the existence of neutral curves with double minima (one quasi-periodic and the other subharmonic). Table 1 shows the wavenumber and frequency values at which these minima occur. Note that for a quasi-periodic branch there are two incommensurate onset frequencies ω_{QP} the first of which corresponds to

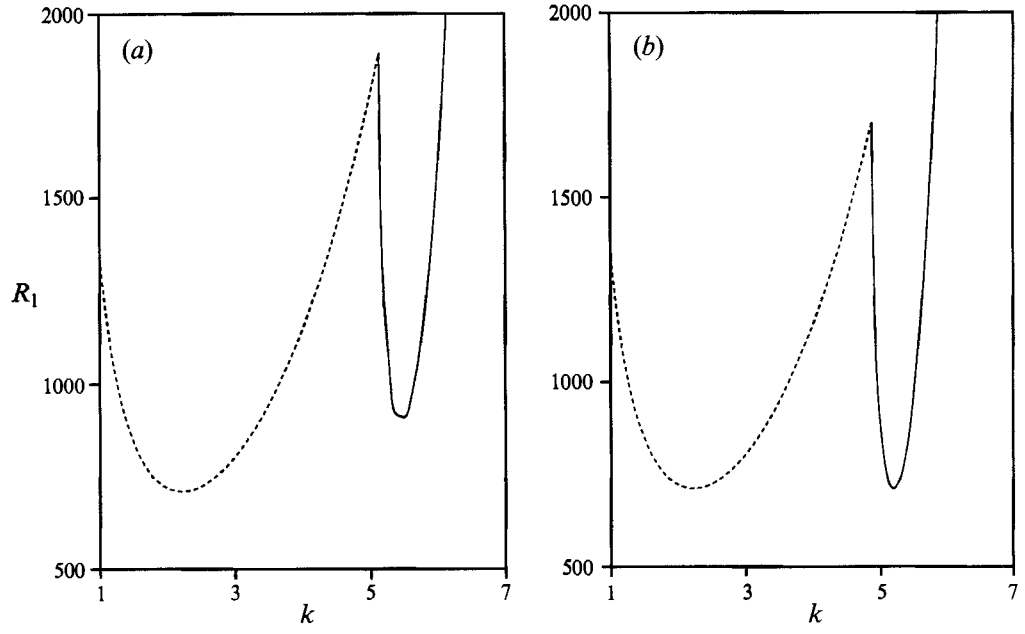

FIGURE 5. Neutral curves for a gravity-modulated stress-free doubly diffusive layer in the liquid-metal range. $Pr = 10^{-2}$, $\gamma_{22} = 3 \times 10^{-4}$, $f = 1$, $h = 0.1$, $\Omega = 10$. – – –, Quasi-periodic branch; ——, subharmonic branch. (*a*) $R_2 = -3300$, (*b*) $R_2 = -3387.52$. In (*b*) the two onset frequencies which occur at the same $R_{1,crit} = 711.3$ are: $\omega = 3.353$ at $k_{c1} = 2.23$ and $\omega = 5$ at $k_{c2} = 5.21$.

the imaginary part of the characteristic exponent α_I and the second one to the dimensionless modulation frequency Ω. In figure 5(*a*) the critical Rayleigh number belongs to a quasi-periodic neutral curve that bifurcates into a subharmonic curve at $k = 5.1544$. For a slightly different value of R_2, an even more interesting situation is shown in figure 5(*b*), namely the occurrence of two incommensurate wavenumbers at two incommensurate onset frequencies at the same critical Rayleigh number. For this special combination of parameters, a temporally and spatially quasi-periodic bifurcation from the basic state is possible. In figure 5(*b*), the quasi-periodic/subharmonic bifurcation point occurs at $k = 4.9223$.

With rigid boundaries, figure 6(*a*, *b*) displays the same topology as figure 5(*a*, *b*), namely a bifurcating subharmonic branch. It is evident that the value of R_2 for which two different wavenumbers at two different frequencies at the same critical Rayleigh number occur lies in between the R_2 values from figures 6(*a*) and 6(*b*). Therefore, the temporally and spatially quasi-periodic onset behaviour is also found in the case of rigid boundaries at a higher value of R_2 than that for the free–free case. Another consequence of the existence of the subharmonic branch in figures 5 and 6, is a discontinuous change in the lengthscale of the convection cells ($\lambda_s = 2\pi d/k_{crit}$) for continuous variations of R_2. For a 3% variation of R_2, the critical wavenumbers in figures 6(*a*) and 6(*b*) are 3.37 and 5.83, respectively, implying a reduction of almost half in the width of the convection cells.

In all neutral curves where a subharmonic curve branches out from a quasi-periodic curve, the values of the imaginary parts of the critical characteristic exponent α_I coincide at the bifurcation point. For example, the quasi-periodic branch in figure 5(*a*) starts with $\alpha_I = 1.734$ at $k = 1$, increases monotonically, and ends at the bifurcation point $k = 5.151$ with a value of $\alpha_I = 5$ which is exactly half the frequency of the

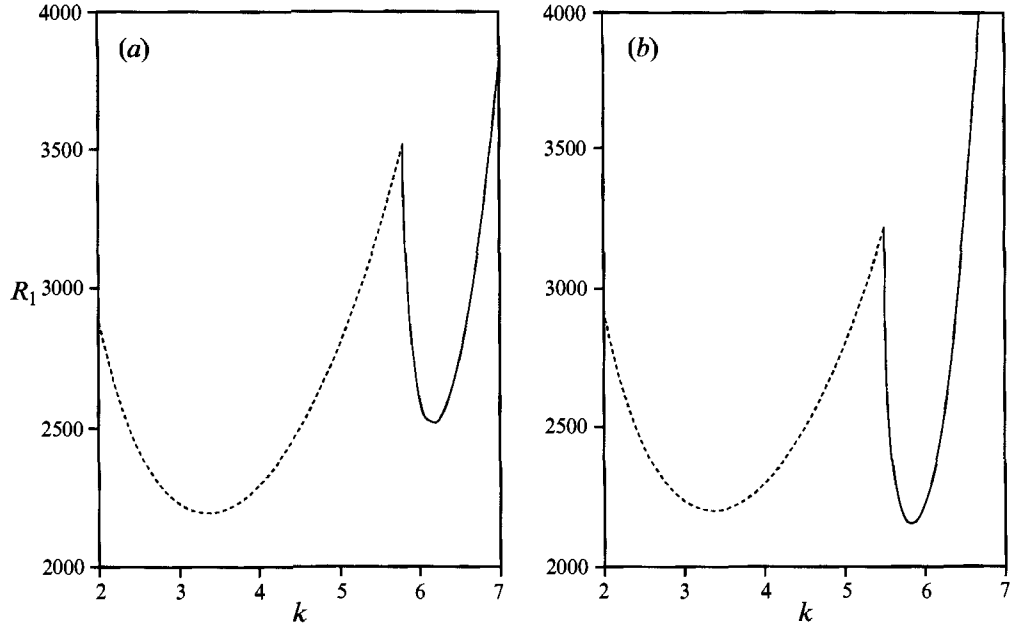

FIGURE 6. Neutral curves for a gravity-modulated doubly diffusive layer in the liquid-metal range with rigid boundaries. $Pr = 10^{-2}$, $\gamma_{22} = 3 \times 10^{-4}$, $f = 1$, $h = 0.1$, $\Omega = 10$. – – –, Quasi-periodic branch; ——, subharmonic branch. (*a*) $R_2 = -3200$, (*b*) $R_2 = -3300$.

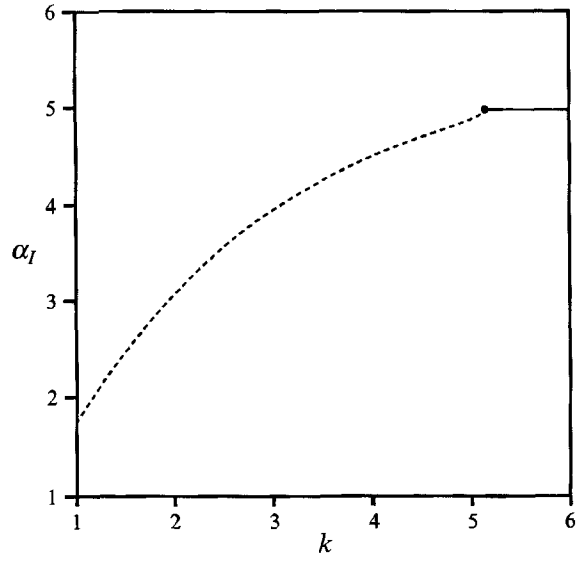

FIGURE 7. Imaginary part of the most unstable characteristic exponent (α_I) as a function of wavenumber (k) for a stress-free doubly diffusive liquid-metal layer. $Pr = 10^{-2}$, $\gamma_{22} = 3 \times 10^{-4}$, $R_2 = -3300$, $f = 1$, $h = 0.1$, $\Omega = 10$. – – –, Quasi-periodic branch; ——, subharmonic branch; •, quasi-periodic/subharmonic bifurcation point.

modulation. At this bifurcation point, the subharmonic curve commences (see figure 7) and the value of α_I remains constant along this branch. Numerical computations in the liquid-metal range show the location of the quasi-periodic/subharmonic bifurcation point(s) being displaced to the left in the (R_1, k)-plane as R_2 becomes more

negative. The shifting of the bifurcation point(s) to the left is accompanied by a lowering of the subharmonic extremum and a narrowing of the subharmonic neutral curve, with no appreciable change in the extremum of the quasi-periodic neutral curve. This situation makes it possible for the subharmonic extremum to meet the quasi-periodic extremum at the same critical Rayleigh number, thereby allowing quasi-periodic onset in time and in space to take place.

The effects of gravity modulation on the stability criteria in the case of stress-free boundaries were also compared with constant-gravity configurations, for which analytical solutions can be obtained (see Appendix). In the liquid-metal range, the imaginary parts of the temporal eigenvalues of the unmodulated problem are almost identical to the imaginary parts of the characteristic exponents of the modulated problem with the same thermophysical properties. By incorporating into the dispersion relation for unmodulated doubly cross-diffusive convection the claim that subharmonic disturbances originate when the value of α_I along the quasi-periodic branch reaches $\frac{1}{2}\Omega$, we obtain explicitly an expression applicable to modulated fluid layers. Therefore, in the limit $Pr \ll 1$, $\gamma_{22} \ll 1$, and $\gamma_{12} \ll 1$, a necessary condition for the existence of a subharmonic branch which bifurcates from a quasi-periodic neutral curve is

$$-Pr\,R_2 > \tfrac{1}{4}\Omega^2. \tag{4.1}$$

At leading order, the approximate location of the quasi-periodic/subharmonic bifurcation point is given by

$$k_{QPSH} = \frac{\pi\Omega}{(4Pr(-R_2)-\Omega^2)^{\frac{1}{2}}} + O(\delta), \tag{4.2}$$

where the perturbation parameter is

$$\delta = \frac{\gamma_{21}(Pr+\gamma_{22})}{1+\gamma_{21}}.$$

The validity of (4.1) can be easily verified with the parameters for figure 5(*a*, *b*). Calculations of the quasi-periodic/subharmonic bifurcation point using (4.2) for the values in figures 5(*a*) and 5(*b*) give wavenumber locations at 5.5536 and 5.2727, respectively. These results are 7.2% and 6.6% different from the actual values, respectively.

For the dimensionless parameters used in figure 6(*a*, *b*), we estimated typical temperature differences (ΔT) between the upper and lower layers based on liquid-metal data given by Webber and Stephens (1968) for a mean gravity of 1 mg and an amplitude of 0.1 mg. In these cases, critical thermal Rayleigh numbers are on the order of 2000. For layers 2 cm and 3 cm deep, $\Delta T = 1250$ °C, 370 °C, respectively. The corresponding dimensional frequencies are on the order of 10^{-1} Hz, which have been observed in microgravity environments (Nelson 1991).

4.3. *Imposed doubly cross-diffusive stratification*

Figure 8 shows the effect of the cross-diffusion coefficient γ_{21} in a stability boundary $(R_1)^{\frac{1}{5}}$ as a function of $(-R_2)^{\frac{1}{5}}$ for typical parameters in the liquid-metal range (fifth roots of the Rayleigh numbers are used to highlight salient features in the region near the origin). In this case, cross-diffusion has an appreciable influence only on the synchronous onset, while the subharmonic and quasi-periodic boundaries are hardly affected. The boundary of convective stability resembles that of an unmodulated doubly diffusive layer (Turner 1974); however, values of $-R_2$ beyond the quasi-

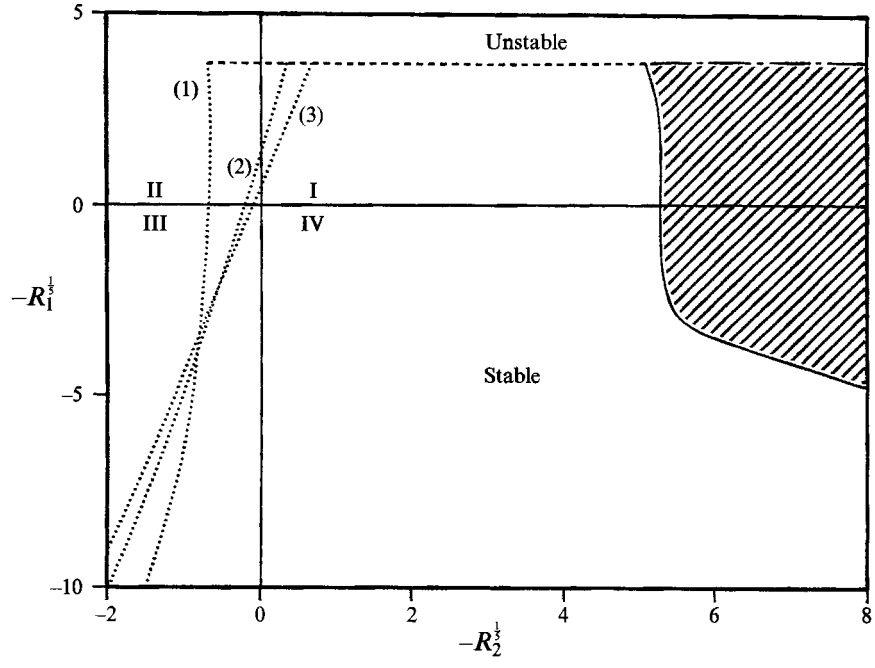

FIGURE 8. Stability boundary for a gravity-modulated doubly cross-diffusive layer in the liquid-metal range with stress-free boundaries. $Pr = 10^{-2}$, $\gamma_{22} = 3 \times 10^{-4}$, $f = 1$, $h = 0.1$, $\Omega = 10$. (1) $\gamma_{21} = 2.25 \times 10^{-4}$, (2) $\gamma_{21} = 0$, (3) $\gamma_{21} = -2.25 \times 10^{-4}$. · · · · ·, Synchronous branch; – – –, quasi-periodic branch; ——, subharmonic branch.

periodic/subharmonic bifurcation make the layer very unstable (a feature not possible in the unmodulated layer). In the absence of modulation, the shaded area in figure 8 becomes a stable region (the chain-dotted line is part of the unmodulated stability boundary which corresponds to oscillatory onset). The appearance of this shaded region indicates that for certain parameter combinations, the effect of modulation is destabilizing and could be dangerous if convection has to be avoided. Notice from figure 8 that a negative (positive) γ_{21} causes the layer to become more stable (unstable) for finger-like configurations (third quadrant) but more unstable (stable) for very weak diffusive-like configurations (first quadrant). When γ_{21} is negative, the location of the synchronous/quasi-periodic bifurcation point lies in the diffusive-like region whereas a sufficiently positive γ_{21} causes this point to lie in the second quadrant of the stability boundary.

Disconnected subharmonic neutral curves can be found in some parameter ranges in either stress-free or rigid boundary configurations. Figure 9(*a–d*) shows the effect of including various cross-diffusion coefficients on neutral stability curves for the following parameters: $Pr = 7$, $\gamma_{22} = 0.8$, $R_2 = -2000$, $\Omega = 20$, $f = 1$, $h = 1$. These parameters were chosen to illustrate the effect of cross-diffusion and are not data from any particular system. Figure 9(*b*, *c*) shows a disconnected subharmonic neutral curve whose extremum determines the critical Rayleigh number. Figure 9(*c*, *d*) shows the effect of changing the sign of the Dufour coefficient (γ_{12}) while maintaining all other parameters fixed. A positive Dufour coefficient makes the subharmonic disconnected neutral curve disappear, causing the layer to become more stable. Note that the most stable configuration of figure 9 corresponds to figure 9(*d*) which has a positive Dufour coefficient and a negative Soret coefficient.

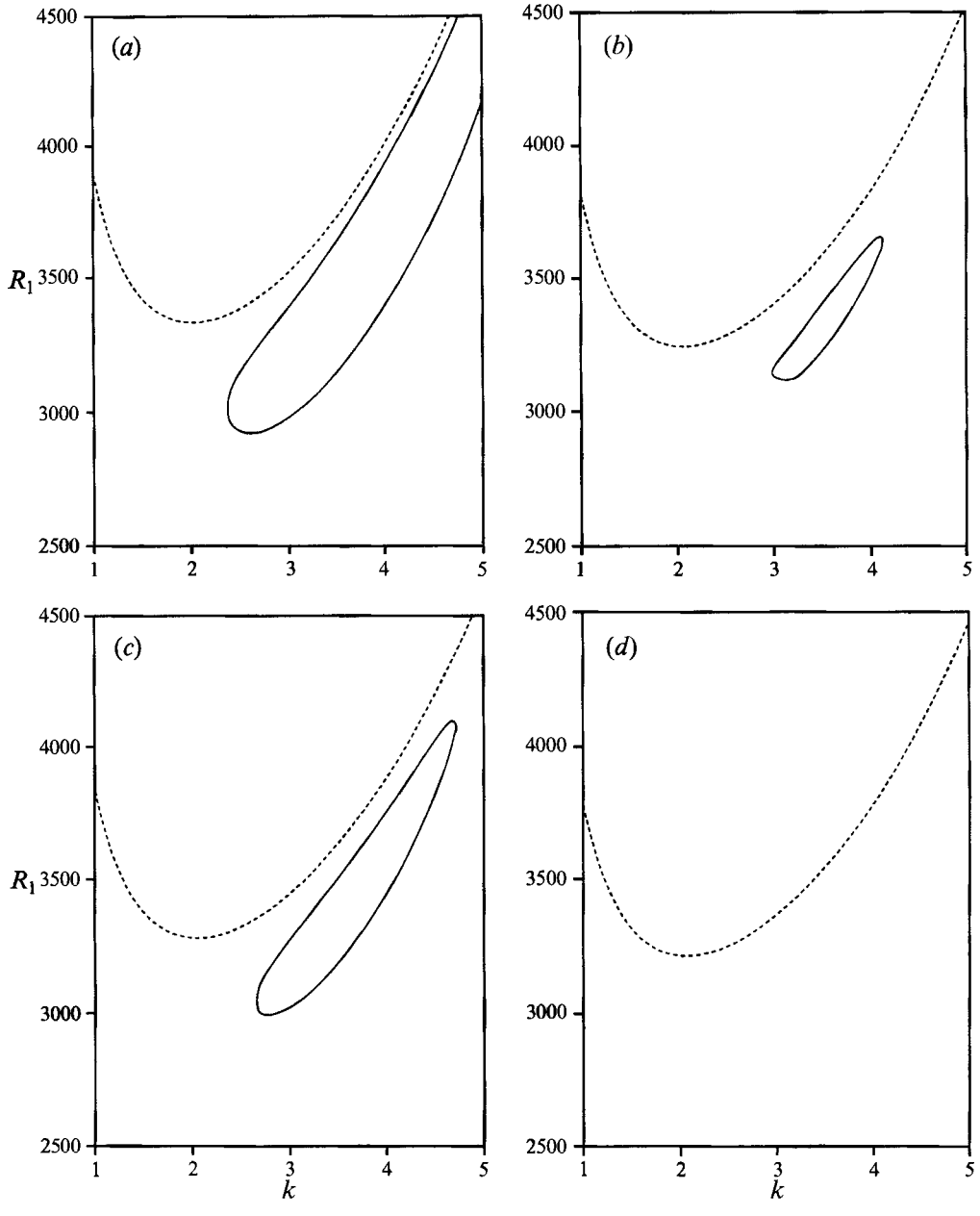

FIGURE 9. Sequence of neutral curves showing the effect of various cross-diffusion coefficients on a gravity-modulated stress-free doubly diffusive layer. $Pr = 7$, $\gamma_{22} = 0.8$, $R_2 = -2000$, $f = 1$, $h = 1$, $\Omega = 20$. ----, Quasi-periodic branch; ——, subharmonic branch. (*a*) $\gamma_{12} = 0$, $\gamma_{21} = 0$, (*b*) $\gamma_{12} = 0$, $\gamma_{21} = -1.6 \times 10^{-2}$, (*c*) $\gamma_{12} = -10^{-2}$, $\gamma_{21} = -1.6 \times 10^{-2}$, (*d*) $\gamma_{12} = 10^{-2}$, $\gamma_{21} = -1.6 \times 10^{-2}$.

Figure 10 shows the analogue of the rigid boundaries from figure 9(*b*) with the same properties except that $R_2 = -3200$. The extrema occur at a higher value than that of figure 9(*b*) since rigid boundaries stabilize the layer.

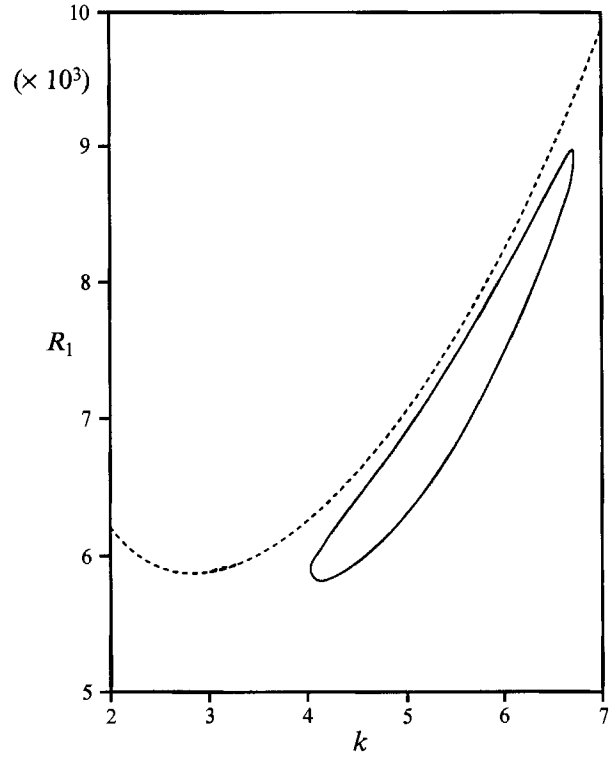

FIGURE 10. Neutral curve for a gravity-modulated doubly cross-diffusive layer with rigid boundaries. $Pr = 7$, $\gamma_{22} = 0.8$, $R_2 = -3200$, $f = 1$, $h = 1$, $\Omega = 20$, $\gamma_{12} = 0$, $\gamma_{21} = -1.6 \times 10^{-2}$. ----, Quasi-periodic branch; ——, subharmonic branch.

4.4. *Induced doubly diffusive stratification*

As pointed out by Praizey (1986), the Soret effect in molten alloys may cause the solute to migrate to either the hot or cold boundary, depending on the system and the solute concentration. Thus, in the liquid-metal range, Soret numbers can be either positive or negative. In this subsection, we construct a stability boundary in the range $-1 \leqslant Sr \leqslant 1$.

Figure 11(*a*) shows a typical neutral curve when in a modulated stress-free layer a solute gradient is induced by Soret separation. In figure 11(*a*) the negative Soret number induces a diffusive-like stratification which causes the appearance of a finite range of linearly stable Rayleigh numbers. This stable range is bounded above by a quasi-periodic branch and below by a synchronous branch. The seemingly straight lower boundary of the stability range has a maximum negative Rayleigh number near $k = \pi/\sqrt{2}$, however, its radius of curvature is much greater than that of the upper quasi-periodic boundary.

For values of the Soret number greater than a certain critical (negative) value, the lower synchronous curve disappears yielding the usual semi-infinite range for R_1. A similar topology is recovered for rigid boundaries as shown in figure 11(*b*). However, the finite range of stability almost triples the stable range found in the case of stress-free boundaries for the same Soret number. Figure 12 shows the stability boundary $(R_1)^{\frac{1}{3}}$ as a function of Sr. This curve is reminiscent of that reported by Hurle & Jakeman (1971) and Platten & Legros (1984) for an unmodulated layer. A distinguishing feature

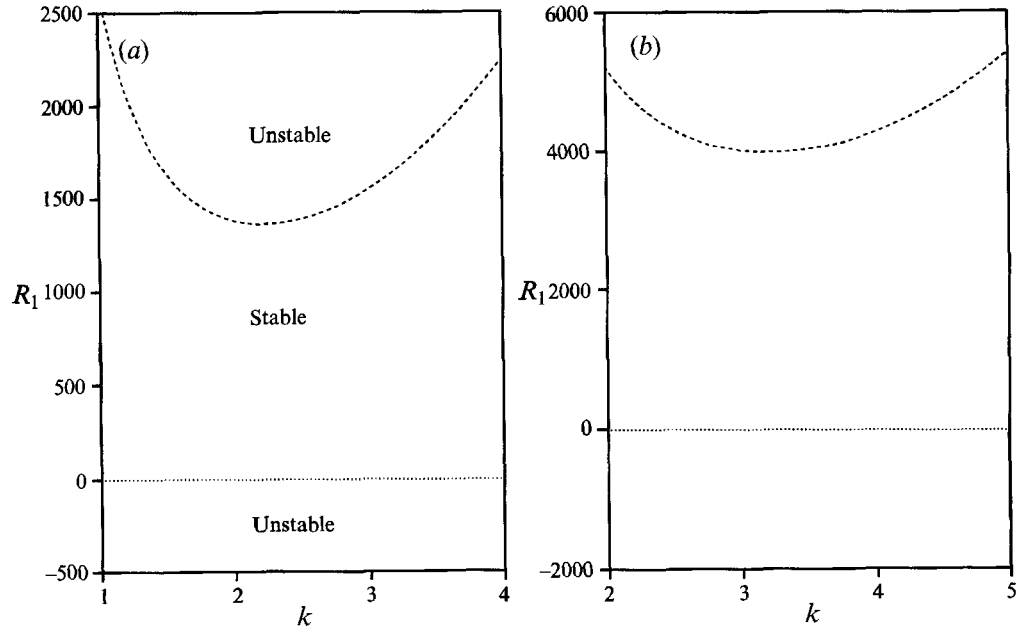

FIGURE 11. Neutral curve for a gravity-modulated Soret-induced solute distribution. $Sr = -0.5$, $Pr = 10^{-2}$, $\gamma_{22} = 3 \times 10^{-4}$, $f = 0.5$, $h = 1$, $\Omega = 50$. · · · · ·, Synchronous branch; ——, quasi-periodic branch. (*a*) Stress-free boundaries, (*b*) rigid boundaries.

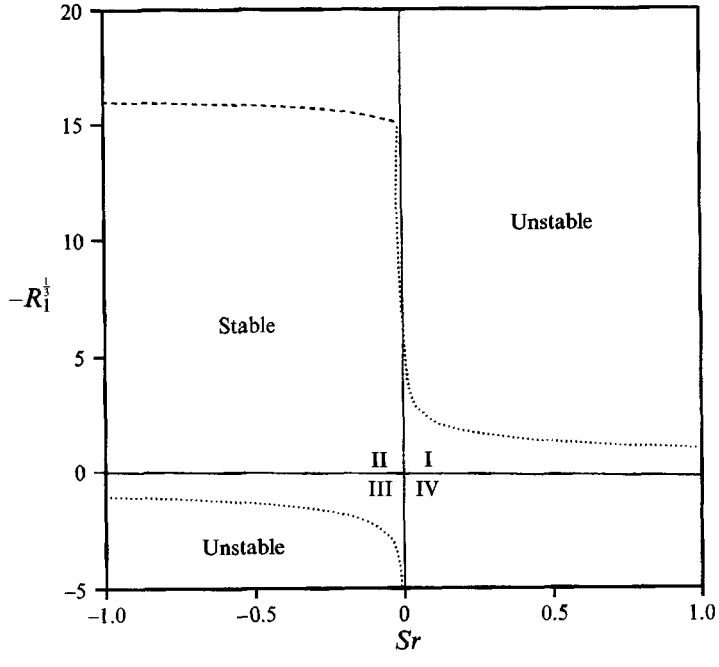

FIGURE 12. Stability boundary for a gravity-modulated Soret-induced solute distribution with rigid boundaries. $Pr = 10^{-2}$, $\gamma_{22} = 3 \times 10^{-4}$, $f = 0.5$, $h = 1$, $\Omega = 50$. · · · · ·, Synchronous branch; ——, quasi-periodic branch.

is the convex quasi-periodic branch in the second quadrant of the stability boundary in contradistinction to the concave oscillatory branch found in the unmodulated case. For this particular parameter vector no subharmonic branches were found. An extended search of neutral curves for higher wavenumber values, showed the existence of subharmonic branches whose extrema did not contribute to the stability criteria.

5. Conclusions

By varying the stratification and boundary conditions and systematically analysing the relative localization of the various neutral curves, we determined the stability criteria for several fluid layer configurations. Gravity modulation in doubly-cross diffusive systems modifies substantially the onset of convective instability of fluid layers when compared to their unmodulated counterparts. The topology of neutral curves is more complex than that encountered in constant-gravity multiply diffusive layers. This is due not only to the large number of parameters required to establish the stability criteria, but also to the existence of quasi-periodic marginally stable curves (in addition to synchronous and subharmonic).

A striking feature is a set of parameters for which a subharmonic branch bifurcates from a quasi-periodic neutral curve. For stress-free layers, a necessary condition for the existence of a subharmonic/quasi-periodic bifurcation and an expression for the wavenumber location at which it occurs were derived and verified within the liquid-metal range. In this parameter range, neutral curves with double minima were found. The implications of such an event occurring in both stress-free and rigid boundaries are: (i) an abrupt jump in the lengthscale of the convection cells for continuous variations of R_2; (ii) for increasingly stable solute stratification in diffusive-like configurations, there is a critical solutal Rayleigh number beyond which the layer becomes increasingly unstable via subharmonic disturbances; and (iii) the existence of two incommensurate onset frequencies at two incommensurate wavenumber for the same critical Rayleigh number, thus leading to a temporally and spatially quasi-periodic bifurcation from the basic state. Additional features not possible in the absence of modulation are: (i) neutral curves exhibiting multiple bifurcation points connecting three different classes of asymptotically stable solutions; (ii) connected and closed disconnected subharmonic neutral curves. This latter feature indicates a strong sensitivity of the extrema locations (in the (R_1, k)-plane) to small variations in the cross-diffusion coefficients.

We thank the kind assistance of Tzay-Fa Su for performing some computations. We also thank Patrick S. Lowery for helpful suggestions on an earlier draft of this paper. This work is based in part on the PhD dissertation of the first author (Terrones 1991). Some of the results were presented at the 30th AIAA Aerospace Sciences Meeting in Reno, Nevada, January 1992. The financial support provided by NASA Microgravity Science and Applications Division through Grant NAG-1268 is gratefully acknowledged.

Appendix

The equations that follow are valid for stress-free doubly diffusive systems under a constant gravity field. First, we consider a doubly cross-diffusive layer in which the gradients of two stratifying agencies are independently imposed. Second, we consider Soret-driven solute stratification by a temperature gradient.

A.1. *Imposed gradients*

There is only one critical wavenumber for steady and oscillatory onset:

$$k_c = \pi/\sqrt{2}.$$

The Rayleigh number above which the layer is unstable with respect to steady onset is given by

$$R_{1,S} = \frac{1}{\gamma_{22}-\gamma_{21}}\left[(\gamma_{22}-\gamma_{12}\gamma_{21})\frac{(\pi^2+k^2)^3}{k^2}-(1-\gamma_{12})R_2\right],$$

and with respect to oscillatory onset is

$$R_{1,O} = \frac{1}{1+Pr+\gamma_{21}}\left[(1+\gamma_{22})\left(1+Pr+\gamma_{22}+\frac{\gamma_{22}-\gamma_{21}\gamma_{12}}{Pr}\right)\frac{(\pi^2+k^2)^3}{k^2} - (Pr+\gamma_{22}+\gamma_{12})R_2\right].$$

The dispersion relation is

$$(\pi^2+k^2)^2\{Pr[\gamma_{21}(1-\gamma_{12})-\gamma_{22}(\gamma_{22}-\gamma_{21})]-(\gamma_{22}-\gamma_{21})(\gamma_{22}-\gamma_{12}\gamma_{21})\} = \frac{k^2}{\pi^2+k^2}(1-\gamma_{22}+\gamma_{21}-\gamma_{12})PrR_2+(1+Pr+\gamma_{21})\omega^2$$

where ω is the onset frequency.

A.2. *Soret convection*

The only critical wavenumber is the same as in §A.1. We assume that R_1 (based on the temperature gradient) is imposed and R_2 (based on the solute gradient) is induced according to

$$R_2 = SrR_1.$$

Note that our definitions for the Rayleigh numbers are related to more conventional definitions through

$$R_{\text{Thermal}} = R_1, \quad R_{\text{Solutal}} = -R_2/\gamma_{22}.$$

For steady onset we have

$$R_{1,S} = \frac{1}{1+Sr(1+1/\gamma_{22})}\frac{(\pi^2+k^2)^3}{k^2},$$

and for oscillatory onset

$$R_{1,O} = \frac{(1+\gamma_{22})(1+Pr)(1+\gamma_{22}/Pr)}{1+Pr(1+Sr)}\frac{(\pi^2+k^2)^3}{k^2}.$$

The dispersion relation is

$$\frac{Sr[\gamma_{22}(1+Sr)-1](1+\gamma_{22})(1+Pr)(\gamma_{22}+Pr)}{1+Pr(1+Sr)}-\gamma_{22}[PrSr+\gamma_{22}(1+Sr)(1+Pr)] = \frac{(1+Pr-\gamma_{22}Sr)\omega^2}{(\pi^2+k^2)^2}.$$

REFERENCES

BIRINGEN, S. & PELTIER, L. J. 1990 Numerical simulation of the 3-D Bénard convection with gravitational modulation. *Phys. Fluids* A **2**, 754–764.

CHANDRASEKHAR, S. 1961 *Hydrodynamic and Hydromagnetic Stability*. Clarendon.

DE GROOT, S. R. 1952 *Thermodynamics of Irreversible Processes*. North-Holland.

GERSHUNI, G. Z., ZHUKHOVITSKII, E. M. & IURKOV, I. S. 1970 On convective stability in the presence of periodically varying parameter. *J. Appl. Math. Mech.* **34**, 442–452.

GRESHO, P. M. & SANI, R. L. 1970 The effects of gravity modulation on the stability of a heated fluid layer. *J. Fluid Mech.* **40**, 783–806.

HENRY, D. 1990 Analysis of convective situations with the Soret effect. In *Low Gravity Fluid Dynamics and Transport Phenomena* (ed. J. N. Koster & R. L. Sani), pp. 437–485. AIAA.

HURLE, D. T. J. & JAKEMAN, E. 1971 Soret-driven thermosolutal convection. *J. Fluid Mech.* **47**, 667–687.

LOPEZ, A. R., ROMERO, L. A. & PEARLSTEIN, A. J. 1990 Effect of rigid boundaries on the onset of convective instability in a triply diffusive fluid layer. *Phys. Fluids* A **2**, 897–902.

MCDOUGALL, T. J. 1983 Double-diffusive convection caused by coupled molecular diffusion. *J. Fluid Mech.* **126**, 379–397.

MCFADDEN, G. B., RHEM, R. G., CORIELL, S. R., CHUCK, W. & MORRISH, K. A. 1984 Thermosolutal convection during directional solidification. *Metall. Trans.* **15A**, 2125–2137.

MURRAY, B. T., CORIELL, S. R. & MCFADDEN, G. B. 1991 The effect of gravity modulation on solutal convection during directional solidification. *J. Cryst. Growth* **110**, 713–723.

NELSON, E. S. 1991 An examination of anticipation g-jitter on space station and its effects on materials processes. *NASA TM* 103775.

PEARLSTEIN, A. J., HARRIS, R. M. & TERRONES, G. 1989 The onset of convective instability in a triply diffusive fluid layer. *J. Fluid Mech.* **202**, 443–465.

PLATTEN, J. K. & LEGROS, J. C. 1984 *Convection in Liquids*. Springer.

PRAIZEY, J. P. 1986 Thermomigration in liquid metallic alloys. *Adv. Space Res.* **6**, 51–60.

SAUNDERS. B. V., MURRAY, B. T., MCFADDEN, G. B., CORIELL, S. R. & WHEELER, A. A. 1992 The effect of gravity modulation on thermosolutal convection in an infinite layer of fluid. *Phys. Fluids* A **4**, 1176–1189.

TERRONES, G. 1991 Gravity modulation and cross-diffusion effects on the onset of multicomponent convection. PhD dissertation, University of Arizona.

TERRONES, G. 1993 Cross-diffusion effects on the stability criteria in a triply diffusive system. *Phys. Fluids* A **5** (to appear).

TERRONES, G. & PEARLSTEIN, A. J. 1989 The onset of convection in a multi-component fluid layer. *Phys. Fluids* A **1**, 845–853.

TURNER, J. S. 1974 Double-diffusive phenomena. *Ann. Rev. Fluid Mech.* **6**, 37–56.

TURNER, J. S. 1985 Multicomponent convection. *Ann. Rev. Fluid Mech.* **17**, 11–44.

WADIH, M. & ROUX, B. 1988 Natural convection in a long vertical cylinder under gravity modulation. *J. Fluid Mech.* **193**, 391–415.

WADIH, M., ZAHIBO, N. & ROUX, B. 1990 Effect of gravity jitter on natural convection in a vertical cylinder. In *Low Gravity Fluid Dynamics and Transport Phenomena* (ed. J. N. Koster & R. L. Sani), pp. 309–352. AIAA.

WEBBER, G. M. B. & STEPHENS, R. W. B. 1968 Transmission of sound in molten metals. In *Physical Acoustics*, vol. IV-B (ed. W. P. Mason), pp. 53–97. Academic.

WHEELER, A. A., MCFADDEN, G. B., MURRAY, B. T. & CORIELL, S. R. 1991 Convective stability in the Rayleigh–Bénard and directional solidification problems: High-frequency gravity modulation. *Phys. Fluids* A **3**, 2847–2858.

YAKUBOVICH, V. A. & STARZHINSKII, V. M. 1975 *Linear Differential Equations with Periodic Coefficients*. John Wiley and Sons.